Sequential development of synapses in dendritic domains during adult neurogenesis

Wolfgang Kelsch*†, Chia-Wei Lin*†, and Carlos Lois*†‡§

*Picower Institute for Learning and Memory, †Department of Brain and Cognitive Science, and ‡Department of Biology, Massachusetts Institute of Technology, 77 Massachusetts Avenue, Cambridge, MA 02139

Communicated by Fernando Nottebohm, The Rockefeller University, Millbrook, NY, September 8, 2008 (received for review October 25, 2007)

During the process of integration into brain circuits, new neurons develop both input and output synapses with their appropriate targets. The vast majority of neurons in the mammalian brain are generated before birth and integrate into immature circuits while these are being assembled. In contrast, adult-generated neurons face an additional challenge as they integrate into a mature, fully functional circuit. Here, we examined how synapses of a single neuronal type, the granule cell in the olfactory bulb, develop during their integration into the immature circuit of the newborn and the fully mature circuit of the adult rat. We used a genetic method to label pre and postsynaptic sites in granule neurons and observed a stereotypical development of synapses in specific dendritic domains. In adult-generated neurons, synapses appeared sequentially in different dendritic domains with glutamatergic input synapses that developed first at the proximal dendritic domain, followed several days later by the development of input-output synapses in the distal domain and additional input synapses in the basal domain. In contrast, for neurons generated in neonatal animals, input and input-output synapses appeared simultaneously in the proximal and distal domains, respectively, followed by the later appearance of input synapses to the basal domain. The sequential formation of synapses in adult-born neurons, with input synapses appearing before output synapses, may represent a cellular mechanism to minimize the disruption caused by the integration of new neurons into a mature circuit in the adult brain.

bulb | dendrite

Integration of new neurons continues throughout life in the adult mammalian olfactory bulb (OB) (1, 2). During the process of integration into brain circuits, new neurons develop both input and output synapses with their appropriate targets. Whereas the majority of neurons in the olfactory bulb integrate into an immature circuit while it is being assembled, neurons generated in adulthood face an additional challenge as they integrate into a mature, fully functional circuit. In particular, the formation of synapses by a new neuron in a functioning circuit may interfere with circuit operation and, thus, it could result in maladaptive behaviors. Additionally, it is still not known whether new neurons integrating into the neonatal and adult olfactory system have the same or different functions in the circuit and, therefore, adult- and neonatal-generated neurons could employ different modes of integration. To compare how new neurons are added to neonatal and adult circuits, we examined the pattern of synapse development of a single neuronal type, the granule cell (GC) in the olfactory bulb, during its integration into the immature circuit of the newborn and the mature circuit of the adult rat.

The majority of neurons added to the OB of adult rats are GC neurons. GCs are axonless inhibitory interneurons that have both a basal dendrite and an apical dendrite (Fig. 1*A*). The apical dendrite can be divided into an unbranched segment emerging from the soma followed by a branched segment (distal domain). The basal dendrite (basal domain) and unbranched apical dendrite receive axo-dendritic glutamatergic input from axon collaterals of the OB's projection neurons and from the olfactory cortices (3–6). The distal domain of the apical dendrite has bidirectional dendro-dendritic synapses present in spines where input and output synapses are colocalized and functionally coupled. These bidirectional synapses receive glutamatergic input synapses from the lateral dendrites of the OB's projection neurons and release GABA back onto these projection neurons (7). These dendro-dendritic synapses in the distal domain are the exclusive output of GCs, and are responsible for local inhibition of the projection neurons in the olfactory bulb (7–9). Activation of axo-dendritic input sites in the basal domain and the unbranched apical dendrite is thought to globally excite the GCs, thus facilitating recurrent dendro-dendritic inhibition in the distal domain (8, 9).

To visualize the development and distribution of input and output synaptic sites in entire GCs, we labeled their progenitors with genetic markers localized specifically to synapses. To visualize glutamatergic input synapses, we expressed a PSD-95:GFP fusion protein. PSD-95 is a scaffolding protein that localizes to the postsynaptic density of glutamatergic synapses (10) and has been extensively used as a postsynaptic marker of glutamatergic synapses (11–14). PSD-95 is present in virtually all GC glutamatergic synapses, where it is restricted to clusters in the postsynaptic density (15), is already highly expressed at birth (16), and appears early during assembly of the postsynaptic density (15). To label presynaptic synapses (output synapses), we used a synaptophysin:GFP fusion protein. Synaptophysin:GFP was the first synaptic vesicle protein to be cloned and has been extensively used to study the distribution and density of presynaptic sites in neurons both *in vitro* and *in vivo* (17–22).

We labeled progenitors for GC neurons with these genetic markers to visualize their synapse development, and observed that in adult-generated neurons, PSD-95:GFP-positive clusters (PSD^+C) developed initially at high density in the proximal 15% of the unbranched apical dendrite. We therefore defined the proximal 15% of the unbranched apical dendrite as the proximal domain. In contrast, PSD^+Cs in the basal domain only developed later together with PSD^+Cs in the distal domain. The late development of PSD^+Cs in the distal domain was tightly coupled to the development of output synapses as labeled by synaptophysin:GFP^+ clusters (Syp^+C) in the same domain. In contrast, neonatal-generated GCs developed PSD^+Cs and Syp^+Cs in the distal domain simultaneously to PSD^+Cs in the proximal and before those in the basal domain. These observations revealed that new GCs in an adult brain environment follow a pattern of integration that differs from that during the initial circuit assembly when most GCs are generated. The sequential formation of synapses in adult-born neurons, with proximal input

Author contributions: W.K., C.-W.L., and C.L. designed research; W.K., C.-W.L., and C.L. performed research; W.K., C.-W.L., and C.L. contributed new reagents/analytic tools; W.K., C.-W.L., and C.L. analyzed data; and W.K. and C.L. wrote the paper.

The authors declare no conflict of interest.

Freely available online through the PNAS open access option.

§To whom correspondence should be addressed. Massachusetts Institute of Technology, 46–5255, 43 Vassar Street, Cambridge, MA 02139. E-mail: loisc@mit.edu.

This article contains supporting information online at www.pnas.org/cgi/content/full/0807970105/DCSupplemental.

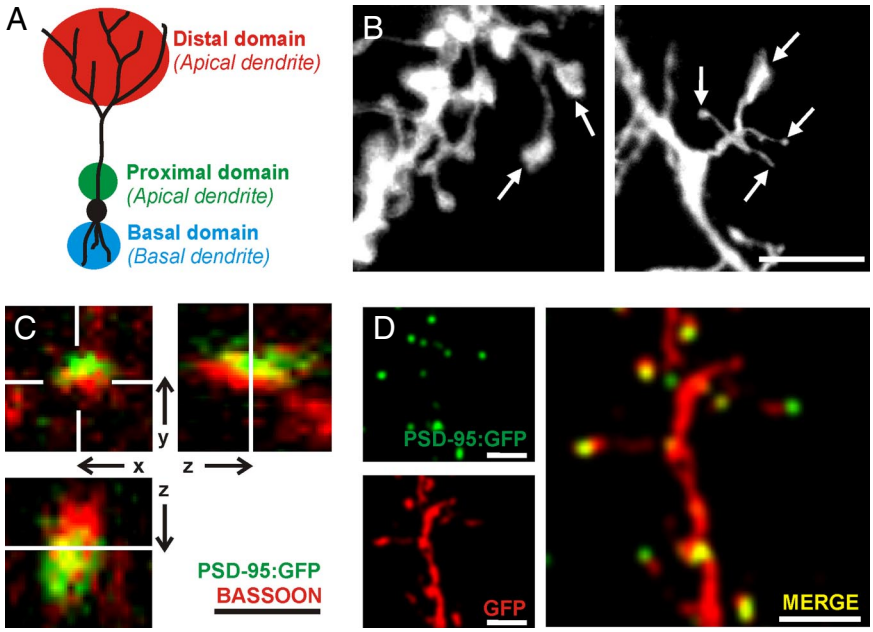

Fig. 1. Glutamatergic input to dendritic domains and PSD-95:GFP positive clusters (PSD$^+$Cs) *in vivo*. (*A*) GCs have different dendritic domains: a basal domain (= basal dendrite) and different domains in the apical dendrite. The apical dendrite divides into an unbranched segment emerging from the soma followed by a more distal branched segment (= distal domain). Because we observed a high density of glutamatergic input synapses in the proximal 15% of the unbranched apical dendrite, we defined it as the proximal domain. (*B*) Branched spines with several spine heads and filopodia-like protrusions in a GFP labeled adult-generated GC 28 d.p.i. (Scale bar, 5 μm.) (*C*) Confocal 3D image shows a PSD$^+$C in a new GC that is contacted by the presynaptic marker, bassoon (bar, 1 μm.) (*D*) In GCs expressing PSD-95:GFP, PSD$^+$C could be detected by direct intrinsic fluorescence as green clusters. The dendritic morphology of the GC was revealed by amplification the low levels of PSD-95:GFP in the cytoplasm (that could not be detected by intrinsic fluorescence) with immunofluorescence against GFP (red). The merged images of PSD$^+$C (intrinsic fluorescence in green) and dendritic morphology (immunofluorescence against GFP in red) allowed attributing PSD$^+$Cs to specific dendritic domains of identified GCs (Scale bar, 5 μm.)

synapses appearing before output synapses, may represent a cellular adaptation to minimize the disruption caused by the integration of new neurons into a functioning circuit.

Results

Development of Glutamatergic Synaptic Input Sites. The aim of the present study was to examine the development of glutamatergic input and inhibitory output synapses of new GCs in the OB of newborn and adult animals. In some types of neurons, glutamatergic synaptic input is exclusively found in dendritic spines (23). However, spine counting was not appropriate to determine the distribution of glutamatergic synapses in GCs as their spines are frequently branched (Fig. 1*B*) (24), and some of their glutamatergic synapses are directly located in the dendritic shaft, not associated with spines (24). To visualize the development and distribution of glutamatergic synapses we genetically labeled postsynaptic densities with a GFP-tagged PSD-95 construct (PSD-95:GFP).

We first determined whether PSD-95:GFP delivered to progenitor cells with retroviruses was an appropriate method to label for postsynaptic sites. Indeed, PSD-95:GFP-positive clusters (PSD$^+$Cs) were restricted to synapses and overlapped with endogenous PSD-95 expression (supporting information (SI) Fig. S1 *C* and *D*). In addition, retroviral expression of PSD-95:GFP did not change the strength and number of glutamatergic synapses in cultured neurons (*SI Text*, Fig. S1 *E*–*G*).

All dendritic domains of GCs born in adulthood (including the basal, proximal and distal domain) received functional glutamatergic synaptic input (*SI Text*, Fig. S1 *A* and *B*) (4, 25), and distal glutamatergic input synapses are colocalized with GABAergic output synapses in the distal domain with a 1:1 stoichiometry (7, 24, 26). PSD$^+$Cs in GCs were in tight apposition to the presynaptic marker bassoon *in vivo* (Fig. 1*C*), indicating that PSD$^+$Cs indeed revealed postsynaptic sites of synapses. To attribute PSD$^+$Cs to a particular GC, we took advantage of the presence of low levels of diffuse PSD-95:GFP protein in the cytoplasm not detectable by its endogenous fluorescence (Fig. 1*D*). This diffuse PSD-95:GFP protein could be visualized by amplifying its signal with antibodies raised against GFP (coupled to a red fluorophore to distinguish it from the intrinsic green fluorescence of PSD$^+$Cs) and allowed us to attribute PSD$^+$Cs to a dendritic arbor belonging to a particular GC.

In adult animals, almost no PSD$^+$Cs were detected at 10 days post infection (d.p.i.) when most GCs had just completed their migration and started to extend their dendritic arbors (Fig. 2*A*). PSD$^+$Cs started to appear in the proximal dendritic domain ≈14 d.p.i. after the initial formation of the dendritic tree (Fig. 2*B*). These PSD$^+$Cs at the proximal domain reached their final density at 17 d.p.i., when few PSD$^+$Cs had appeared at the basal or distal domains. At the basal and distal domains PSD$^+$Cs reached their final density only at a later time point (28 d.p.i.; Fig. 2*B*). We quantified the density of PSD$^+$Cs in the different dendritic domains of new GCs (Fig. 3*A*) and observed that PSD$^+$Cs at the proximal domain indeed developed first, followed by PSD$^+$Cs at the basal and distal domains (for statistical analysis see *SI Text*). The PSD$^+$Cs first detected at 14 d.p.i. are likely to represent true synapses, as these PSD$^+$Cs were contacted by the presynaptic marker bassoon (Fig. S2*C*). In 94% of our GC sample (n = 151), the density of PSD$^+$Cs in the proximal domain was several fold higher than the density in the entire unbranched apical dendrite throughout maturation (Fig. 3*A*). Maturation of synapses over time was paralleled by an increase in the mean fluorescent area of PSD$^+$Cs (Fig. S2*B*). Four weeks after the birth of the new neurons, the density of PSD$^+$Cs stabilized and revealed no significant changes in the dendritic domains between 28 and 56 d.p.i. We did not quantify PSD$^+$Cs

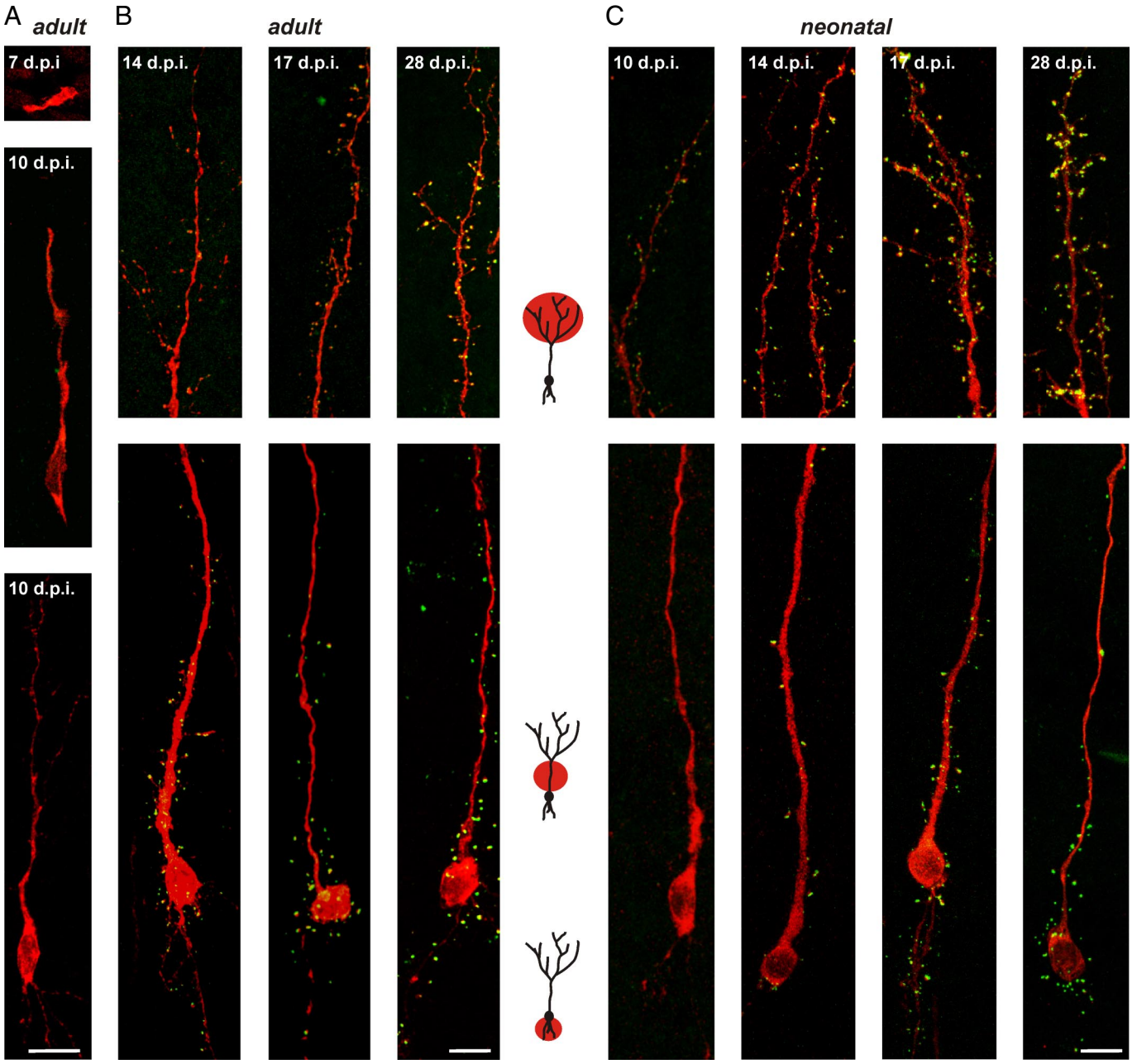

Fig. 2. Development of PSD$^+$Cs during maturation of adult- and neonatal-generated GCs. (*A*) In adult-generated superficial GCs, no PSD$^+$Cs were detectable during migration (7 d.p.i.) and the initial extension of the dendritic arbor (10 d.p.i.) (Scale bar, 10 μm.) *B* and *C* show the development of PSD$^+$Cs at different d.p.i. The *Upper* row shows the distal domain and the *Lower* row the basal domain and the unbranched segment of the apical dendrite with the proximal domain of a GC. (*B*) Only at later time points (14, 17, and 28 d.p.i.) PSD$^+$Cs developed during maturation of adult-generated GCs. PSD$^+$Cs were first observed in high density in the proximal domain followed by PSD$^+$Cs at the distal domain (Scale bar, 10 μm.) (*C*) In neonatal-generated superficial GCs PSD$^+$Cs developed simultaneously in the proximal and distal domains during maturation of neonatal-generated GCs at 10, 14, 17, 28 d.p.i. (Scale bar, 10 μm.)

at the soma as their presence and density was highly variable (data not shown).

Whereas adult-generated GCs integrate into a mature, functioning circuit, GCs generated in the neonatal period integrate into a circuit that is still developing. To investigate whether the appearance of synapses in new GCs differs between neonatal and adult animals, we examined the development of PSD$^+$Cs in neonatal-generated GCs (Figs. 2*C* and 3*C*). PSD$^+$Cs appeared in neonatal-generated GCs $\approx$10–14 d.p.i., after they had extended their dendritic arbors. In contrast to the situation described for adult neurogenesis, neonatal-generated GCs acquired glutamatergic synapses simultaneously in the proximal and distal domains of their apical dendrite followed by later development of glutamatergic synapses to the basal domain (Figs. 2*C* and 3*C*; for statistical analysis see *SI Text*).

The distal dendritic domain of GCs can either branch deep and superficial in the external plexiform layer where GCs then contact different types of projection neurons (7, 27). However, the sequential development of PSD$^+$Cs was the same for deep and superficial GCs in adult-born neurons (*SI Text*, Fig. 3 vs. Fig. S2). Similarly, we observed that both deep and superficial GCs generated in newborn animals had a synchronous synaptic

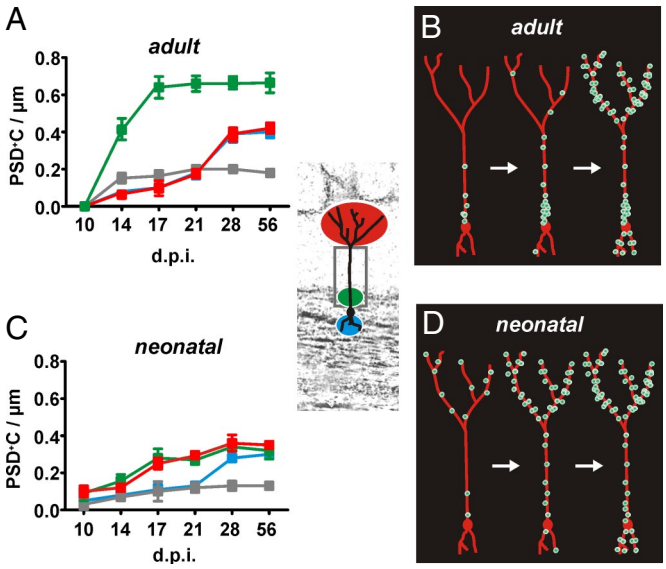

Fig. 3. Domain-specific development of PSD$^+$Cs during maturation of adult- and neonatal-generated GCs (with branching in the superficial external plexiform layer). (*A*) Mean PSD$^+$C density at different stages (d.p.i.) during the maturation of new GCs generated in adult animals. The dendritic domains are indicated in the graph: basal (blue), proximal (green), and distal domain (red line) as well as the entire unbranched apical dendrite (gray). (*B*) The diagram illustrates the developmental pattern of PSD$^+$Cs during maturation of adult-generated GCs. (*C*) Mean PSD$^+$C density at different stages (d.p.i.) during the maturation of new GCs generated in newborn animals. (*D*) The diagram illustrates the developmental pattern of PSD$^+$Cs during maturation of neonatal-generated GCs.

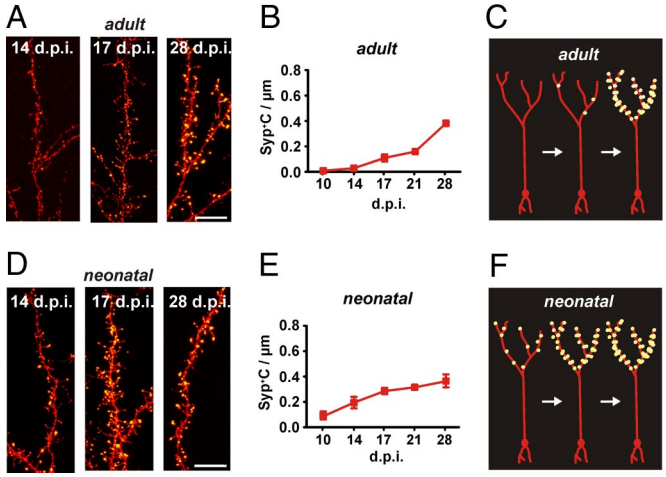

Fig. 4. Development of synaptophysin:GFP-positive clusters (Syp$^+$Cs) during maturation of adult- and neonatal-generated GCs (with branching in the superficial external plexiform layer). (*A*) In adult-generated GCs, Syp$^+$Cs developed during maturation of adult-generated GCs in the distal domain (14, 17, 28 d.p.i.; Scale bar, 10 μm.) (*B*) Mean Syp$^+$C density at different stages (d.p.i.) during the maturation of new GCs generated in adult animals. (*C*) The diagram illustrates the developmental pattern of Syp$^+$Cs during maturation of adult-generated GCs. (*D*) In neonatal-generated GCs Syp$^+$Cs developed earlier than in adult-generated GCs (*A*) in the distal domain (14, 17, and 28 d.p.i.; Scale bar, 10 μm.) (*E*) Mean Syp$^+$C density at different stages (d.p.i.) during the maturation of new GCs generated in neonatal animals. (*F*) The diagram illustrates the developmental pattern of Syp$^+$Cs during maturation of neonatal-generated GCs.

development of proximal axo-dendritic and distal dendro-dendritic input (*SI Text*, Fig. 3 vs. Fig. S2).

In summary, in adult-generated GCs, the proximal axo-dendritic input domain developed first, and was followed by the appearance of PSD$^+$Cs in the distal dendro-dendritic and basal domains (Fig. 3*B*). In contrast, GCs generated in the neonatal period developed PSD$^+$Cs first in their proximal and distal domains (Fig. 3*D*), and later in the basal domain.

Development of Synaptic Output Sites in New GCs. We wondered whether the delayed development of PSD$^+$Cs in the distal domain of adult generated GCs compared with those generated in the neonatal period was paralleled by a delayed development of the distal output synapses. Ultrastructural studies of dendro-dendritic synapses of GCs have revealed that the glutamatergic input synapses and GABAergic output synapses exist in tight spatial coupling with a 1:1 stoichiometry in spines of the distal domain (26). During embryonic development, the mitral-to-GC input synapse develops first, followed within a day by the GC-to-mitral cell output synapse (26). We investigated the development of the presynaptic output sites in GCs by using synaptophysin:GFP as a genetic marker for the presynaptic vesicle release machinery. The only output synapses of GCs are located in their dendro-dendritic synapses and, as expected, synaptophysin:GFP positive clusters (Syp$^+$Cs) were only found in the distal domain of GCs (Fig. 4 and Fig. S3*C*).

To examine the development of output synapses in GCs we used retroviruses encoding synaptophysin:GFP and followed the procedures described for PSD$^+$Cs. We observed that the development of Syp$^+$Cs in the distal domain was delayed in adult-generated GCs when compared with neonatal-generated GCs (compare Fig. 4 *A* and *D*). Similar to our observations for the development of PSD$^+$Cs in the distal domain of adult-generated GCs (compare Fig. 3*A*), we observed that Syp$^+$Cs in the distal domain were sparse at 17 d.p.i. and reached their final density only at 28 d.p.i. (Fig. 4*B*, for statistical analysis see *SI Text*). In contrast, neonatal-generated GCs developed Syp$^+$Cs in the distal domain from early on (14 d.p.i.) (Fig. 4*E*) as described above for PSD$^+$Cs (compare Fig. 3*C*, for statistical analysis, see *SI Text*). This observation was independent of whether GCs had deep or superficial dendrites (*SI Text*; Fig. S3).

In summary, the development of Syp$^+$Cs, as markers for presynaptic output sites, closely paralleled the maturation of PSD$^+$Cs as markers of postsynaptic input sites in the distal domain (compare Fig. 3 *B* and *D* to Fig. 4 *C* and *F*). These observations reveal that the development of dendro-dendritic synapses is delayed compared with the input synapses at the proximal domain of adult-generated GCs, but not in neonatal-generated GCs.

Discussion

We observed that adult-generated GCs in the mammalian OB develop their presynaptic and postsynaptic sites sequentially in different dendritic domains. In particular, comparing the proximal dendritic domain to the distal domain revealed significant differences in the appearance of synapses. The development of glutamatergic synaptic sites at the proximal domain preceded the development of dendro-dendritic input and output synapses in the distal domain by several days. This observation suggests that adult-generated neurons integrate into the olfactory circuits by first developing input synapses that can control their global excitation before developing distal input-output synapses that mediate recurrent inhibition within the bulb, that is, the new neurons "listen" before they "speak."

A recent study on murine adult-generated GCs based on immunocytochemical staining also suggested a delayed development of the distal dendritic domain (28). However, this study did not provide any quantification of the dynamics of synaptic maturation and did not detect any special pattern of synaptic development in the proximal domain. Our method, based on

genetic labeling of presynaptic and postsynaptic sites, allowed us both to quantify the dynamics of synaptic maturation in complete cells and to measure the density of synaptic sites. Our measurements reveal a unidentified pattern of synapse development in adult-born neurons, with a low density of synapses in the basal and distal domains at a time when the proximal domain already contains a high density of input synapses.

Different Properties of Adult- and Neonatal-generated Neurons. All dendritic domains of GCs receive input synapses that are glutamatergic and therefore excitatory, while the output synapses are GABAergic and therefore inhibitory. The basal and proximal domain receive axo-dendritic glutamatergic input whereas the distal domain receives dendro-dendritic glutamatergic input and releases GABA with its recurrent output synapse (see also above). Axo-dendritic input synapses originating either from axon collaterals of OB's projection neurons or from centrifugal projections of the olfactory cortex (5, 29) were first formed on the proximal domain of GCs born in adulthood. Axo-dendritic input can evoke action potentials (8, 9) that then spread throughout dendrites to cause Ca^{2+} influx in the spines of GCs (30). This global excitation can then facilitate the release of GABA at the dendro-dendritic synapses in the distal domain, thus mediating inhibition of the OB projection neurons (8, 9). This latter consequence, however, only happens after the dendro-dendritic synapses of the GCs' distal domain are in place and thus enable the new neurons to shape odor discrimination (31). This order, in which the axo-dendritic synapses on the proximal domain are formed first, followed by formation of the dendro-dendritic synapses in the distal domain, ensures that control of global excitation precedes the origination of the inhibitory synaptic output signals that constitute the main task of the OB's GCs. The sequential acquisition of proximal axo-dendritic input, before the dendro-dendritic input and output, could provide a unique form of plasticity for adult-generated GCs, not present during initial circuit assembly. In line with the different timing in the appearance of axo-dendritic input in the proximal domain compared with the distal dendro-dendritic synapses, adult- and neonatal-generated neurons also differ in the time course in which they start generating action potentials. Neonatal-generated neurons can fire fast action potentials around the time when they finish migrating whereas most adult-generated GCs only develop the ability to spike two weeks after they are born (our unpublished observations in rats) (32) at the time when proximal synapses develop, but before distal synapses emerge. Thus, in adult-generated neurons, the input to the proximal domain, which appears around the time when the neuron gained the ability to fire action potentials, could control the global activity of the new neuron before its dendro-dendritic input-output synapses mature in the distal domain. This observation suggests that adult-generated GCs may integrate silently in the circuit as they will only develop output synapses after they acquired many other functions, like their proximal input synapses and the ability to spike. In contrast, input synapses, as well as the ability to spike, appeared simultaneously to output synapses in neonatal-generated GCs, suggesting that no 'silent' mode of integration is required. It is interesting to note that for neurons born both in neonatal and adult animals, axo-dendritic glutamatergic synapses developed in all cases in two steps, first in the proximal and later in the basal domain. The development of axo-dendritic input in two steps may provide additional excitatory drive to tune their activity. Future studies will reveal whether basal and proximal axo-dendritic input comes from different sources (e.g., centrifugal cortical projections vs. local axon collaterals from OB's projection neurons) and serves different functions.

In addition, the timing of the appearance of glutamatergic input into the proximal dendritic domain could be important to regulate both the integration and survival of new neurons into the circuits of the olfactory bulb. Whereas most of the postmigratory new neurons added into the bulb of newborns survive (33), only half of these neurons generated in the adult stably integrate and survive (33, 34). Interestingly, the peak of adult-generated GC death (33, 34) occurs between the time when glutamatergic synapses first appear in the proximal domain and when these new neurons reach their final density of distal input-output synapses. The main period of cell death thus precedes the development of output synapses in adult-generated neurons. This again suggests that the initial steps of integration of adult-generated neurons into the circuit occur "silently" before output synapses have appeared. Thus, neonatal- and adult-generated GCs use different strategies for their integration into the olfactory circuit. Additionally, these different strategies of integration could satisfy the demands of olfactory processing which change from neonatal to adult life (35).

Influence of Brain Maturation on Synapse Formation by New Neurons. The different patterns of synapse development in neonatal- and adult-generated neurons could either be because of different intrinsic properties of the new neurons or to differences in the maturation of the brain circuit into which the new neurons integrate. It is possible that postnatal changes in the structure or function of axon terminals ending at GCs may result in different patterns of synaptic appearance in new GCs, and thus, could explain why axo-dendritic input does not develop before distal dendro-dendritic synapses in neonatal-generated GCs. However, axon terminals from the olfactory cortex ending at the GCs are already functional one week after birth (4, 36), thus preceding the maturation of the neonatal-generated GCs that we studied. In addition, excitatory synapses in the proximal domain preceded those formed on the basal domain even though these two domains both receive axo-dendritic inputs. This observation again suggests that the sequential acquisition of axo-dendritic input to specific dendritic domains in newly generated GCs cannot be solely explained by the maturational state of the brain. Future experiments exposing new GCs generated in newborn and adult animals to different environments by heterochronic transplantation might elucidate the respective contributions of brain maturation and cell-intrinsic properties for the specific patterns of synaptic development.

Minimizing the Disruption of Brain Function Caused by the Integration of New Neurons in Sequential Steps. Sequential development of synapses in adult-generated GCs may represent a cellular mechanism to minimize the potential disruption caused by the integration of new neurons into a functioning circuit. Whereas the proximal axo-dendritic input is thought to control the global excitability of GCs, the distal domain contains the only output synapses of these neurons. Thus, the pattern of sequential synaptic development in the adult olfactory bulb may allow control of the new neuron's activity before it can influence the performance of other cells. Interestingly, adult neurogenesis also occurs in motor systems (37). Sequential "silent" integration of new neurons followed by output activation could provide a mechanism by which the brain can recruit new neurons with minimal disruption of existing functions. The sequential incorporation of afferent control and synaptic output could be a key component of successful neuronal integration during adulthood. If our interpretation is correct, then this input-output relation may have to be approached carefully when using neuronal replacement to treat neurological disorders.

Materials and Methods

Generation of Retroviral Vectors. We replaced the ubiquitin-C promoter region of FUGW, a self-inactivating lentiviral vector derived from HIV-1, with a regulatory sequence −570 to −93 bp from the transcription start site of the

human synapsin gene to produce a construct called HsynGW. The cDNA of PSD-95:GFP was a fusion protein with GFP at the C terminus (38). PSD-95:GFP was amplified by PCR and inserted into HsynGW replacing GFP (called HsynPSD95g). Recombinant HsynPSD95g virus was prepared and stored as described (39). To visualize spine morphology we used an oncoretroviral vector derived from Moloney Leukemia virus with an internal promoter derived from the LTR from the Rous Sarcoma Virus (RSV) driving palmitoylated GFP (called MRSVPalmG). To visualize glutamatergic postsynaptic clusters or presynaptic release sites, we generated a vector called MRSVPSD95g or MRSVSypg by replacing the palmitoylated GFP from MRSVPalmG with the ORF of PSD95:GFP or Synaptophysin:GFP, respectively.

Stereotaxic Injections. All animal procedures were approved by the local Animal Welfare Committee. Stereotactic injections of retroviral vectors were performed into the subventricular zone of SD rats of either sex (Charles River) (for details see *SI Text*).

Tissue Processing and Immunohistochemistry. For each time point after viral infection, three rats were given an overdose of ketamine/xylazine and perfused transcardially with PBS at 37°C for 30 s followed by 3 min of 3% PFA. Fifty-μm thick coronal slices were cut and incubated in primary rabbit anti-GFP (1:4.000, Chemicon) or anti-bassoon (1:750) antibodies at 4°C overnight, and Alexa-555 secondary antibodies (1:750, Molecular Probes) diluted in blocking for 2 h at RT.

Confocal Microscopy. Confocal image stacks were acquired by using an Olympus Fluoview confocal microscope (60× oil-immersion lens (NA, 1.4), Olympus) (pixel size, 0.23 × 0.23 μm), and with z-step 0.25 μm. A typical image stack consisted of approx. 80–150 image planes each of 1024 × 1024 pixels. For each stack, laser intensity and detector sensitivity were set to the same values determined in initial experiments.

Image Processing and Quantification. After acquisition, maximal intensity projections were prepared for each image stack by using the MetaMorph analysis software (Universal Imaging). No filtering was generally necessary. For the projection images the threshold was set so that any possible diffuse GFP fluorescence at the dendritic shaft was below this threshold. The number of PSD-95:GFP$^+$ clusters (PSD$^+$C) in a region of interest was counted by using the integrated morphometry analysis function of the MetaMorph software. The length of the respective segment of the dendritic arbor was then measured and the density of PSD$^+$Cs was determined. All datasets were manually supervised to prevent the inclusion of unspecific green fluorescence. The total number of PSD$^+$Cs analyzed was 48,657. Dendritic length was not corrected for shrinkage because of tissue processing and 2D projection (estimated error up to 15%). To determine whether the late appearance of PSD$^+$Cs at the basal and distal domains was because of setting a threshold for PSD$^+$Cs, we reanalyzed data with a lower threshold. With a lower threshold, the absolute PSD$^+$C density was slightly higher, but the pattern of PSD$^+$C development persisted (Fig. S4*B*), and was therefore not because of differences in PSD$^+$Cs area in the respective dendritic domain. Syp$^+$Cs were analyzed with the same procedure as described for PSD$^+$Cs (total number of Syp$^+$Cs analyzed 15,389). Each data point (e.g., superficial dendritic branching, adult-born, basal domain, 14 d.p.i.) contained normally distributed PSD$^+$C densities from 14 cells. The first time point that we examined for statistical analysis was 14 d.p.i. We used a three-way ANOVA followed by a two-way ANOVA and then tested simple effects by using ANOVA.

ACKNOWLEDGMENTS. We thank Timothy Gardner for critically reading the manuscript, Kevin Allen and Alexey Ponomarenko for help with the statistic analysis, and the Sheng lab for helpful suggestions and reagents. This work was supported by the David and Lucille Packard Foundation (C.L.).

1. Luskin MB (1993) Restricted proliferation and migration of postnatally generated neurons derived from the forebrain subventricular zone. *Neuron* 11:173–189.
2. Lois C, Alvarez-Buylla A (1993) Proliferating subventricular zone cells in the adult mammalian forebrain can differentiate into neurons and glia. *Proc Natl Acad Sci USA* 90:2074–2077.
3. Mori K, Kishi K, Ojima H (1983) Distribution of dendrites of mitral, displaced mitral, tufted, and granule cells in the rabbit olfactory bulb. *J Comp Neurol* 219:339–355.
4. Balu R, Pressler RT, Strowbridge BW (2007) Multiple modes of synaptic excitation of olfactory bulb granule cells. *J Neurosci* 27:5621–5632.
5. Luskin MB, Price JL (1983) The topographic organization of associational fibers of the olfactory system in the rat, including centrifugal fibers to the olfactory bulb. *J Comp Neurol* 216:264–291.
6. Davis BJ, Macrides F (1981) The organization of centrifugal projections from the anterior olfactory nucleus, ventral hippocampal rudiment, and piriform cortex to the main olfactory bulb in the hamster: An autoradiographic study. *J Comp Neurol* 203:475–493.
7. Mori K (1987) Membrane and synaptic properties of identified neurons in the olfactory bulb. *Prog Neurobiol* 29:275–320.
8. Chen WR, Xiong W, Shepherd GM (2000) Analysis of relations between NMDA receptors and GABA release at olfactory bulb reciprocal synapses. *Neuron* 25:625–633.
9. Halabisky B, Strowbridge BW (2003) Gamma-frequency excitatory input to granule cells facilitates dendrodendritic inhibition in the rat olfactory Bulb. *J Neurophysiol* 90:644–654.
10. Sheng M (2001) Molecular organization of the postsynaptic specialization. *Proc Natl Acad Sci USA* 98:7058–7061.
11. Niell CM, Meyer MP, Smith SJ (2004) In vivo imaging of synapse formation on a growing dendritic arbor. *Nat Neurosci* 7:254–260.
12. Ebihara T, Kawabata I, Usui S, Sobue K, Okabe S (2003) Synchronized formation and remodeling of postsynaptic densities: Long-term visualization of hippocampal neurons expressing postsynaptic density proteins tagged with green fluorescent protein. *J Neurosci* 23:2170–2181.
13. Washbourne P, Bennett JE, McAllister AK (2002) Rapid recruitment of NMDA receptor transport packets to nascent synapses. *Nat Neurosci* 5:751–759.
14. Gray NW, Weimer RM, Bureau I, Svoboda K (2006) Rapid redistribution of synaptic PSD-95 in the neocortex in vivo. *PLoS Biol* 4:e370.
15. Sassoe-Pognetto M, *et al.* (2003) Organization of postsynaptic density proteins and glutamate receptors in axodendritic and dendrodendritic synapses of the rat olfactory bulb. *J Comp Neurol* 463:237–248.
16. Shu F, *et al.* (2001) Developmental changes in PSD-95 and Narp mRNAs in the rat olfactory bulb. *Brain Res Dev Brain Res* 132:91–95.
17. Nakata T, Terada S, Hirokawa N (1998) Visualization of the dynamics of synaptic vesicle and plasma membrane proteins in living axons. *J Cell Biol* 140:659–674.
18. Pennuto M, Bonanomi D, Benfenati F, Valtorta F (2003) Synaptophysin I controls the targeting of VAMP2/synaptobrevin II to synaptic vesicles. *Mol Biol Cell* 14:4909–4919.
19. Li Z, Murthy VN (2001) Visualizing postendocytic traffic of synaptic vesicles at hippocampal synapses. *Neuron* 31:593–605.
20. Kaether C, Skehel P, Dotti CG (2000) Axonal membrane proteins are transported in distinct carriers: A two-color video microscopy study in cultured hippocampal neurons. *Mol Biol Cell* 11:1213–1224.
21. Meyer MP, Smith SJ (2006) Evidence from in vivo imaging that synaptogenesis guides the growth and branching of axonal arbors by two distinct mechanisms. *J Neurosci* 26:3604–3614.
22. Valtorta F, Pennuto M, Bonanomi D, Benfenati F (2004) Synaptophysin: Leading actor or walk-on role in synaptic vesicle exocytosis? *Bioessays* 26:445–453.
23. Nimchinsky EA, Sabatini BL, Svoboda K (2002) Structure and function of dendritic spines. *Annu Rev Physiol* 64:313–353.
24. Woolf TB, Shepherd GM, Greer CA (1991) Serial reconstructions of granule cell spines in the mammalian olfactory bulb. *Synapse* 7:181–192.
25. Schoppa NE (2006) AMPA/kainate receptors drive rapid output and precise synchrony in olfactory bulb granule cells. *J Neurosci* 26:12996–13006.
26. Hinds JW (1970) Reciprocal and serial dendrodendritic synapses in the glomerular layer of the rat olfactory bulb. *Brain Res* 17:530–534.
27. Kelsch W, Mosley CP, Lin CW, Lois C (2007) Distinct mammalian precursors are committed to generate neurons with defined dendritic projection patterns. *PloS Biol* 5:e300.
28. Whitman MC, Greer CA (2007) Synaptic integration of adult-generated olfactory bulb granule cells: Basal axodendritic centrifugal input precedes apical dendrodendritic local circuits. *J Neurosci* 27:9951–9961.
29. Kishi K, Mori K, Ojima H (1984) Distribution of local axon collaterals of mitral, displaced mitral, and tufted cells in the rabbit olfactory bulb. *J Comp Neurol* 225:511–526.
30. Egger V, Svoboda K, Mainen ZF (2003) Mechanisms of lateral inhibition in the olfactory bulb: Efficiency and modulation of spike-evoked calcium influx into granule cells. *J Neurosci* 23:7551–7558.
31. Laurent G (1999) A systems perspective on early olfactory coding. *Science* 286:723–728.
32. Carleton A, Petreanu LT, Lansford R, Alvarez-Buylla A, Lledo PM (2003) Becoming a new neuron in the adult olfactory bulb. *Nat Neurosci* 6:507–518.
33. Lemasson M, Saghatelyan A, Olivo-Marin JC, Lledo PM (2005) Neonatal and adult neurogenesis provide two distinct populations of newborn neurons to the mouse olfactory bulb. *J Neurosci* 25:6816–6825.
34. Petreanu L, Alvarez-Buylla A (2002) Maturation and death of adult-born olfactory bulb granule neurons: Role of olfaction. *J Neurosci* 22:6106–6113.
35. Moriceau S, Sullivan RM (2006) Maternal presence serves as a switch between learning fear and attraction in infancy. *Nat Neurosci* 9:1004–1006.
36. Schwob JE, Price JL (1984) The development of lamination of afferent fibers to the olfactory cortex in rats, with additional observations in the adult. *J Comp Neurol* 223:203–222.
37. Nottebohm F (1989) From bird song to neurogenesis. *Sci Am* 260:74–79.
38. Hsueh YP, Sheng M (1999) Requirement of N-terminal cysteines of PSD-95 for PSD-95 multimerization and ternary complex formation, but not for binding to potassium channel Kv1.4. *J Biol Chem* 274:532–536.
39. Lois C, Hong EJ, Pease S, Brown EJ, Baltimore D (2002) Germline transmission and tissue-specific expression of transgenes delivered by lentiviral vectors. *Science* 295:868–872.